Eur. J. Biochem. *255*, 628−637 (1998)

Purification and characterization of recombinant *Thermotoga maritima* dihydrofolate reductase

Valérie WILQUET[1], Joe A. GASPAR[4], Monica VAN DE LANDE[4], Mark VAN DE CASTEELE[2,3], Christianne LEGRAIN[1], Elizabeth M. MEIERING[4] and Nicolas GLANSDORFF[1,2,3]

[1] Research Institute CERIA-COOVI, Brussels, Belgium
[2] Microbiologie, Vrije Universiteit Brussel (VUB), Brussels, Belgium
[3] Flanders Interuniversity Institute for Biotechnology, Brussels, Belgium
[4] Department of Chemistry, University of Waterloo, Ontario, Canada

(Received 23 February/15 May 1998) − EJB 98 0256/4

We have overexpressed the gene for dihydrofolate reductase (DHFR) from *Thermotoga maritima* in *Escherichia coli* and characterized the biochemical properties of the recombinant protein. This enzyme is involved in the *de novo* synthesis of deoxythymidine 5′-phosphate and is critical for cell growth. High levels of *T. maritima* DHFR in the new expression system conferred resistance to high levels of DHFR inhibitors which inhibit the growth of non-recombinant cells. The enzyme was purified to homogeneity in the following two steps: heat treatment followed by affinity chromatography or cation-exchange chromatography. Most of the biochemical properties of *T. maritima* DHFR resemble those of other bacterial or eukaryotic DHFRs, however, some are unique to *T. maritima* DHFR. The pH optima for activity, K_m for substrates, and polypeptide chain length of *T. maritima* DHFR are similar to those of other DHFRs. In addition, the secondary structure of *T. maritima* DHFR, as measured by circular dichroism, is similar to that of other DHFRs. Interestingly, *T. maritima* DHFR exhibits some characteristics of eukaryotic DHFRs, such as a basic pI, an excess of positively charged residues in the polypeptide chain and activation of the enzyme by inorganic salts and urea. Unlike most other DHFRs which are monomeric or part of a bifunctional DHFR-thymidylate synthase (TS) enzyme, *T. maritima* DHFR seems to generally form a dimer in solution and is also much more thermostable than other DHFRs. It may be that dimer formation is a key factor in determining the stability of *T. maritima* DHFR.

Keywords: dihydrofolate reductase; *Thermotoga maritima*; thermal stability; purification; expression in *Escherichia coli*.

Thermotoga maritima is a hyperthermophilic and strictly anaerobic eubacterium with an optimal growth temperature of 80 °C [1]. It belongs to the order Thermotogales, a very ancient and apparently slowly evolving order within the Eubacterial kingdom. Thermotogales occupy, together with the order Aquificales, an isolated position in the phylogenetic tree, separated from other branches of this domain ([2, 3] and references therein). *T. maritima* displays several characteristics that are unique among eubacteria ([2] and references therein); the DNA-dependent RNA polymerase is resistant up to 1 μg/ml rifampicin, the membrane contains a characteristic novel ether lipid, the ribosomes are insensitive to the miscoding-inducing action of aminoglycoside antibiotics, and it contains a reverse DNA-gyrase activity. Thus, the study of *T. maritima* is of great interest from an evolutionary point of view. In addition, most proteins from this organism that have been characterized to date are intrinsically thermostable ([4−8] and references therein) and are, therefore, of interest from a biotechnological point of view.

This paper describes studies on dihydrofolate reductase from *T. maritima*. Dihydrofolate reductase (DHFR) is a key enzyme in one-carbon metabolism. It catalyzes the NADPH-dependent reduction of dihydrofolate (H_2-folate). This reaction is a universal requirement for cell growth; it is one of the sequential reactions in the *de novo* synthesis of dTMP which is required for the biosynthesis of DNA. Tetrahydrofolate, the product of the reaction catalyzed by DHFR, is also involved in the biosynthesis of purines and some amino acids such as glycine, methionine and serine [9, 10]. Consequently, DHFR is the target of widely used antifolate drugs which inhibit cell growth [11−14], and the gene for DHFR is often used as a selection or reporter marker ([15−19] and references therein). Due to their biological and medical importance, genes for DHFR have been cloned from a wide range of organisms representing all the major kingdoms [16, 20−24], and the corresponding proteins have been studied extensively in terms of their function, stability and structure [25−29].

The structural gene (*dyrA*) encoding DHFR of *T. maritima* was recently cloned, sequenced and expressed at low levels in *Escherichia coli* [23]. We have now subcloned and over-expressed *T. maritima* DHFR encoding gene *in E. coli* using the

Correspondence to N. Glansdorff, Department of Microbiology, Onderzoekingsinstituut CERIA-COOVI, 1 Av. E. Gryson, B-1070 Brussels, Belgium
Fax: +32 2 526 72 73.
E-mail: ceriair@ulb.ac.be

Abbreviations. DHFR, dihydrofolate reductase; TS, thymidylate synthase; H_2-folate, dihydrofolic acid; DLS, dynamic light scattering; IC_{50}, inhibitor concentration for 50% of maximal activity; IPTG, isopropyl-1-thio-β-D-galactopyranoside.

Enzymes. Dihydrofolate reductase (EC 1.5.1.3); thymidylate synthase (EC 2.1.1.45).

Note. The nucleotide sequence of the *Thermotoga maritima dyrA* gene is available under Genbank accession number X81845.

Table 1. Bacterial strains and plasmids used in this study.

Strain or plasmid	Genotype/description	Source
E. coli strains		
INVαF′	F′ *end*A1 *rec*A1 *hsd*R17 (r_k^-, m_k^+) *sup*E44 *thi*-1 *gyr*A96 *rel*A1 ϕ80*lac*ZΔM15 Δ(*lac*ZYA-*arg*F)U169λ^-	Invitrogen
BL21(DE3)	F^- *hsd* S gal (r_B^-, m_B^-)(lambdacI857, ind-1, Sam7, nin5, lacUV5-T7 gene/1/)	[30]
Plasmids		
pKK223−3	Ap^r expression vector, pBR322 ori	[33]
pTM8	pKK223-3 with 2.5-kb *Hin*dIII insert of *Tt. maritima* chromosome	[23]
pCR2.1	Ap^r, Km^r cloning vector, ColE1 ori, f1 ori, *lac* promoter, *lacZ*α fragment	Invitrogen
pCRTM	*Tt. maritima dyr* A gene, 0.5 kb insert in pCR2.1	this study
pET3a	Ap^r translation vector, pBR322 ori, T7 promoter, gene 10 translation start site	[31]
pTM9	*Tt. maritima dyr* A gene, 0.5 kb *Nde*I/*Bam*HI insert in pET3a	this study

pET3/BL21(DE3) system [30, 31]. In order to gain more insight into the molecular evolution of DHFRs, and into structure/function relationships in this family of enzymes, we have purified the recombinant protein to homogeneity and characterized its biochemical properties.

MATERIALS AND METHODS

Bacterial strains and growth conditions. Plasmids and *E. coli* strains used in this study are listed in Table 1. Bacteria were grown at 37 °C in medium 853 [32] as liquid medium and with 1.5% agar (Difco) as a solid medium. For bacteria containing recombinant plasmids, the media contained also 25 μg/ml ampicillin or 50 μg/ml kanamycin. *E. coli* INVαF′ competent cells from the Original TA Cloning Kit (Invitrogen) were used as hosts during cloning according to the instruction manual supplied by the manufacturer. Expression of *T. maritima* DHFR was carried out in *E. coli* strain BL21(DE3), using a recombinant plasmid derived from the expression vector pET3a [30, 31].

DNA manipulation and analysis. Restriction enzymes, T4 DNA ligase and alkaline phosphatase were purchased from Boehringer Mannheim, and used according to the manufacturer's instructions. All the DNA manipulations and analyses, including small-scale plasmid preparation, restriction enzyme digests, agarose (Boehringer Mannheim) gel electrophoresis, DNA ligation, transformation of *E. coli*, or DNA fragment purification from low-melting-temperature agarose gels (BioRad), followed standard methods [34]. For large-scale preparation of pure plasmid, the Nucleobond AX Kit (Macherey-Nagel) was used as recommended by the manufacturer. The nucleotide sequences of plasmid pTM9 and of plasmid pTM8 were performed by dideoxy chain termination [35] with the T7 DNA Sequencing Kit (Pharmacia). Nucleotide primers flanking the cloned insert (forward and reverse universal primers) and internal oligonucleotide primers (DyrS1, 5′-GAA GAC CTC TTC CAG AG-3′; DyrS2, 5′-CGT CAC TGT CGA ACC GT-3′; DyrS3, 5′-TCC TAT GAC AGC CAC CC-3′; DyrS4, 5′-CCT TCA CTC GTT TTT TT-3′; DyrS5, 5′-ACG GTT CGA CAG TGA CG-3′; DyrS6, 5′-CAA AGG AAA GTA AC-3′; DyrS7, 5′-GGG TGG CTG TCA TAG GA-3′) were used to sequence both strands of the DNA insert. DNA analysis was performed using the Gibco BRL Sequencing System (Life Technologies).

Polymerase chain reaction. The PCR mix for amplifying the *T. maritima* DHFR-encoding gene from pTM8 plasmid contained 200 μM each nucleotide (dATP, dGTP, dTTP, and dCTP), 20 pmol primers Dyr3 (5′-GCC ATA TGG CAA AAG TGA TTT TC-3′) and Dyr4 (5′-GCG GAT CCT TAA CGG TGC GAT TT-3′), 10 mM Tris/HCl, pH 8.3, 50 mM KCl, 1.5 mM $MgCl_2$, 1 ng pTM8 plasmid DNA as template, and 2.5 U Taq DNA polymerase (Boehringer Mannheim)/100 μl solution. The amplification protocol consisted of 5 min at 94 °C, followed by 30 cycles of 0.5 min at 94 °C, 0.5 min at 52 °C and 1 min at 72 °C, followed by 10 min at 72 °C (Programmable Dri-Block PHC-1 from Techne). The PCR product was analysed using a 1.6% agarose gel and visualized under ultraviolet light. Dyr3 starts with a *Nde*I restriction site which overlaps the ATG start codon, while Dyr4 ends in a *Bam*HI restriction site after the TAA stop codon.

Construction of a plasmid for inducible expression of *T. maritima* DHFR. Plasmids are described in Table 1. Pure pTM8 plasmid preparation was used as a template to amplify the *T. maritima dyrA*-coding sequence by PCR (see above). This DNA fragment was directly cloned into pCR2.1 vector using the Original TA Cloning Kit to yield pCRTM plasmid. The 0.5-kb DNA fragment corresponding to *dyrA* was then obtained from pCRTM by *Nde*I and *Bam*HI digestion, and cloned into the pET3a vector. The resulting plasmid, pTM9, carries the *dyrA*-coding sequence under control of the T7 RNA polymerase promoter.

Assay of dihydrofolate reductase activity. The standard reaction mixture contained 0.15 mM NADPH (Boehringer Mannheim), 0.05 mM H_2-folate (Sigma), and 1−10 U enzyme. The mixture was buffered using 40 mM Mes, pH 6.5, and incubated at 37 °C. Enzyme was incubated with H_2-folate and the reaction was initiated by addition of NADPH. The reaction was monitored by recording the absorption decrease at 340 nm using a PU8740 UV/VIS scanning spectrophotometer (Philips), in a temperature-controlled cuvet. The NADPH consumption due to other enzymes in the crude extract was first determined in a control cuvet that contained buffer, enzyme solution, and NADPH, but no H_2-folate. This aspecific NADPH consumption was then subtracted from the total consumption to obtain the DHFR activity.

Absorbance measurements were converted to units of activity (U) using the standard relation that one unit DHFR activity is the amount of enzyme that catalyzes the reduction of 1 μmol NADPH/hour under standard assay conditions. Protein concentrations were measured by the Lowry method [36], using bovine serum albumin as a standard.

Thermal stability analysis. The thermal stability of *E. coli* DHFR and of recombinant *T. maritima* DHFR was determined by heating crude extracts of *E. coli* non-recombinant and recombinant cells for 15 min for a range of temperatures, then assaying residual activity at 37 °C (using standard assay conditions described above). The stability of the pure *T. maritima* DHFR and the effect of extrinsic factors on thermostability were investigated by incubating the pure enzyme at 80 °C for a range of time, in the presence and in the absence of different agents (Table 4). For these experiments, *T. maritima* apo-DHFR was diluted in, and dialyzed against 50 mM potassium phosphate, pH 7.5.

pH dependence of *T. maritima* DHFR activity. The optimal pH for activity was determined at 37 °C in 50 mM Mes, buffered at different pH values (5.75−7.30), for the enzyme in the crude extract as well as for the pure enzyme. In addition, for the partially purified enzyme (heat treatment for 20 min at 80 °C), activity was assayed at 60 °C in 50 mM potassium phosphate, pH 6.20−7.50, or in 50 mM citrate phosphate, pH 5.25−6.70.

These activity measurements could not be monitored in real time using the scanning spectrophotometer because bubbles appeared in the cuvet when the assay was performed at temperatures above 45 °C. For this reason, the reaction mixture was incubated at 37 °C or 60 °C for 10−20 min, and the sample absorbance was then measured at 340 nm and ambient temperature in a spectrophotometer. The rate of consumption of NADPH due to *T. maritima* DHFR was calculated using the appropriate optical blanks incubated in the same way; one blank contained buffer and H_2-folate; the other contained buffer, enzyme solution and NADPH. The blanks were performed in order to measure the background reaction of the substrates.

Kinetic analysis. K_m for both substrates, the inhibitor concentration for 50% of maximal activity (IC_{50}) for methotrexate and trimethoprim and hysteretic behaviour were studied at 37 °C, in 40 mM Mes, buffer pH 6.5. The K_m values were measured on partially purified enzyme whereas other experiments were performed on the pure enzyme.

For measurements of IC_{50}, in order to obtain a linear kinetic trace, the enzyme was incubated for 5 min with the inhibitor solution and NADPH. The reaction was then initiated by adding H_2-folate. For assays involving trimethoprim, which has a low solubility in water, a concentrated stock solution of inhibitor was prepared in methanol. In order to account for the slight decrease in activity caused by the methanol, the control enzyme reactions for this inhibitor were conducted by adding the appropriate amount of methanol to the reaction mixture.

Expression and purification of recombinant *T. maritima* DHFR. Exponentially growing cultures of *E. coli* BL21(DE3) harbouring the pTM9 plasmid were induced with 0.4 mM isopropyl-1-thio-*β*-D-galactopyranoside (IPTG), harvested after 3−4 hours induction, washed in 0.9% NaCl, and sonicated in 40 mM Mes, pH 6.5, for 20 min (Raytheon Sonic Oscillator, 250 W-10 kHz). The extracts were freed of cell debris by centrifugation for 10 min at 17000 *g*. The crude extract was then thermodenatured by incubating at 80 °C for 20 min. Precipitated protein was removed by centrifuging for 10 min at 31000 *g*, resuspended in 40 mM Mes, pH 6.5, and again centrifuged. This step improved the yield of DHFR by recovering additional protein from the precipitate. Supernatants from both centrifugation steps were pooled and applied to a methotrexate-agarose (Sigma) column (Pharmacia XK16/20) equilibrated with 10 mM Mes, pH 6.5. The column was then washed with 200 ml starting buffer followed by 125 ml 200 mM sodium carbonate, pH 10.3. The enzyme was eluted using 5 ml 200 mM sodium carbonate, pH 10.3, containing 2 mg/ml H_2-folate or methotrexate, followed by 30 ml 20 mM sodium carbonate, pH 10.3, and fractions of 4 ml were collected. Fractions containing DHFR activity were combined, dialyzed overnight against 3×2 L 10 mM sodium carbonate, pH 10.3, and concentrated from ≈20 ml to ≈4 ml in an Amicon concentrator (YM-10 membrane). Due to the high affinity of *T. maritima* DHFR for the ligands used in the elution step, they remained bound to the enzyme. The preparations were thus DHFR−H_2-folate complexes when eluting with H_2-folate and DHFR-methotrexate complexes when eluting with methotrexate. The complex DHFR-methotrexate-NADPH was obtained by adding NADPH to a solution of DHFR-methotrexate complex.

Pure *T. maritima* apo-DHFR (i.e. DHFR with no bound ligands) was obtained as described above, except that after heat denaturation, the protein was subjected to cation exchange chromatography instead of affinity chromatography. The partially purified protein was applied to a 4.6 mm×100 mm column of Poros 20 HS resin (Perseptive Biosystems, Inc.) that had been pre-equilibrated in 25 mM Tris/25 mM bisTrispropane, pH 8.0. Due to its high pI, *T. maritima* DHFR binds to the cation-exchange resin under these conditions. A salt gradient of 0−1 M NaCl was then applied to the column, and the activity of eluted fractions was tested. The enzyme eluted as the major peak from the column at ≈400−550 mM NaCl. SDS/PAGE of the eluted fractions revealed that the centre of the peak of eluted *T. maritima* DHFR contained > 95% pure apoprotein.

Mass spectrometry. Purified *T. maritima* apo-DHFR and DHFR−H_2-folate complex were dialyzed against 10 mM ammonium bicarbonate, pH 7.9, then lyophilized. Protein was then redissolved in 50:50 acetonitrile/H_2O (by vol.) containing ≈10% formic acid and subjected to electrospray ionization mass spectrometry using a Quattro II Mass Spectrometer fitted with an electrospray source (MicroMass).

SDS/PAGE. Sodium dodecyl sulfate/polyacrylamide gel electrophoresis was performed using a Pharmacia PhastSystem with discontinuous buffer system and a continuous 8−25% gradient gel. Gels were stained with Coomassie brilliant blue. Protein standards (Pharmacia, 0.5 μg each on the gel) used for estimation of subunit molecular masses were phosphorylase *b* (94 kDa), albumin (67 kDa), ovalbumin (43 kDa), carbonic anhydrase (30 kDa), trypsin inhibitor (20.1 kDa) and *α*-lactalbumin (14.4 kDa).

Isoelectric focusing gel electrophoresis. The isoelectric points of *T. maritima* apo-DHFR and of the complexes DHFR-methotrexate and DHFR-methotrexate-NADPH were determined by IEF gel electrophoresis using the Pharmacia PhastSystem with broad range gels and using the Hoefer Mighty Small II Vertical Gel Electrophoresis Unit with broad-range IEF gels from Novex. Broad range pI markers (Pharmacia) were supplemented with horse heart cytochrome *c* (Sigma) as a high pI marker (pI = 10.3).

Native molecular-mass determination. The molecular mass of *T. maritima* DHFR−H_2-folate complex was determined under native conditions by gel filtration using a Pharmacia FPLC system fitted with a Superose P12 HR 10/30 column in the following buffers: 100 mM sodium carbonate pH 10.3, 40 mM sodium carbonate plus 0.1 M NaCl, pH 10.3, 50 mM potassium phosphate pH 7.5, 100 mM citrate/HCl, pH 4.3, and 40 mM citrate/HCl plus 0.1 M NaCl, pH 4.3. About 50 μg pure DHFR−H_2-folate (in 0.2 ml) was applied to the gel-filtration column that had been equilibrated and calibrated in each buffer using the following standards (Pharmacia, about 100 μg each protein): aldolase (158 kDa), bovine serum albumin (67 kDa), ovalbumin (43 kDa), chymotrypsinogen A (25 kDa) and ribonuclease A (13.7 kDa).

Dynamic light-scattering measurements. The hydrodynamic radius of *T. maritima* apo-DHFR and of the complexes DHFR−H_2-folate and DHFR-methotrexate were measured by dynamic light scattering (DLS). Samples contained ≈5 mg/ml protein in 75 mM potassium phosphate, pH 6.5. The DLS apparatus used in this study is typical of most systems. Light from a 50-mW Nd: YAG laser (model 532-50, Coherent) of wavelength 532.0 nm was focused onto a standard four-sided clear optical cuvette (Helma). The scattered light was collimated by two 400 μm diameter pinholes placed 35 cm apart and detected by a photomultiplier (model 9863, EMI Electronics, Ltd). Photon counting and pulse shaping were performed using a quantum photometer (model 1140, Princeton Applied Research). Final

autocorrelation was performed by an autocorrelator (model 1096, Langley-Ford). The fitting procedures to recover size distributions are detailed by Hallett et al. [37].

Circular dichroism. CD spectra of *T. maritima* apo-DHFR and of DHFR-methotrexate complexes were acquired on a J715 Spectropolarimeter (Jasco). Samples contained 0.5−5 mg/ml protein in 75 mM KH_2PO_4/K_2HPO_4, pH 6.5, and measurements were made at ambient temperature. Secondary-structure analysis of apo-DHFR was performed using the k2d method which uses a Kohonen neural network to extract the secondary structure from circular dichroism spectra at 200−240 nm [38, 39].

RESULTS

***dyrA* gene subcloning.** The recombinant plasmid pTM8 [23], consisting of expression vector pKK223−3 and a 2.5-kb *Hin*dIII fragment of *T. maritima* DNA, carries the incomplete *pyrB* and *gtlD* genes flanking the complete *dyrA* gene. In *E. coli* cells transformed with the pTM8 plasmid, the host and the *T. maritima* DHFR can be easily distinguished because the recombinant protein is unaffected by heat treatments which completely inactivate *E. coli* DHFR.

Since only low levels of recombinant DHFR were obtained using pTM8, the *T. maritima dyrA* gene was subcloned and overexpressed in *E. coli* in order to facilitate further characterization of the protein. This was achieved by first amplifying the coding part of the *dyrA* gene by PCR using pTM8 plasmid as template. The PCR product, ending in *Nde*I and *Bam*HI restriction sites, was then cloned into the pCR2.1 vector (Table 1). Next, the *Nde*I−*Bam*HI subfragment was cloned into the pET3a expression vector, yielding pTM9 plasmid, which was used to transform *E. coli* BL21(DE3) cells. The *Nde*I restriction site was designed to overlap with the ATG start codon so that this would be preceeded by the Shine-Dalgarno sequence of the new vector.

Both strands of the *dyrA* gene on the pTM8 plasmid and on the pTM9 plasmid were sequenced using the dideoxy-chain termination method, in order to confirm that no mutations had been introduced by the *Taq* DNA polymerase during PCR. One mutation was found in the subcloned *dyrA* gene; base T at position 379 was replaced by C. As a consequence, the deduced polypeptide contained a Leu at position 127 rather than a Phe residue. The residue at position 127 is not strictly conserved, but is hydrophobic in many different sequences (for example, Leu in type-III DHFR from *Salmonella typhimurium*, Val in *E. coli* DHFR, and Phe in mammalian DHFRs). Based on sequence alignments of *T. maritima* DHFR with DHFRs whose structures have been determined by X-ray crystallography (*E. coli* DHFR [40], *Lactobacillus casei* DHFR [40] and human DHFR [41, 42]), residue 127 in *T. maritima* DHFR is located in a loop at the periphery of the protein structure, just outside the active site. A conservative mutation at such a location would be unlikely to have a large effect on activity or stability. Thus, the mutant protein has been purified and further characterized.

Enzyme production and resistance to DHFR inhibitors. The specific activity of partially purified *T. maritima* DHFR in heat-treated (20 min at 60 °C) extracts of *E. coli* cells harbouring pTM9 was found to be 130-fold higher than the activity of analogous extracts of cells harbouring pTM8, and there was no detectable activity in similar extracts of non-recombinant cells. Optimum expression was obtained when cultures were induced by IPTG at the beginning of the exponential growth (A_{660} ≈0.35) and harvested after 4 hours of induction. Within 30 min of induction, cell growth ceased and the A_{660} of induced cultures remained approximately constant for several hours (data not shown). In contrast, induction had no effect on the growth of *E. coli* non-recombinant cells. The lag in growth of induced cultures of *E. coli* recombinant cells could indicate that the overproduction of *T. maritima* DHFR from the plasmid monopolizes the transcriptional and translational machinery of *E. coli*, or that this overproduction is toxic.

E. coli recombinant cells were grown in the absence and in the presence of DHFR inhibitors (trimethoprim and methotrexate). Inhibitor was added to a final concentration of 1 mM and at an A_{660} of 0.3, together with IPTG. Whereas wild-type *E. coli* cells stopped growing 3−4 h after addition of inhibitor, the A_{660} of *E. coli* pTM9 cultures followed the same pattern as cultures without inhibitor, except that the lag in growth was longer (data not shown). Resistance to methotrexate was slightly more marked than resistance to trimethoprim suggesting at first sight that trimethoprim might be a more potent inhibitor for the *T. maritima* DHFR (but see kinetic properties).

Table 2. Purification of *T. maritima* DHFR–H_2-folate or DHFR-methotrexate complexes from pTM9 recombinant *E. coli* cells. The thermodenaturation step is heat treatment for 20 min at 80 °C. Enzyme activity was assayed under standard conditions (see Materials and Methods).

Purification step	Total protein	Total activity	Specific activity	Recovery	Purification
	mg	U	U/mg	%	-fold
Crude extract	1037	9292	9.0	100	1.0
Thermo-denaturation	248	7430	30.0	80	3.3
Methotrexate-agarose	36	6240	173	67	19.2

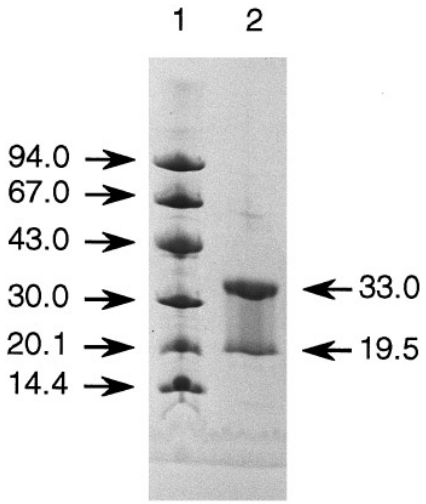

Fig. 1. SDS/PAGE of the purified recombinant dihydrofolate reductase of *T. maritima*. Lane 1, molecular mass markers, 0.5 μg each protein; lane 2, 0.8 μg DHFR. Molecular masses of proteins are in kDa. The gel was stained with Coomassie brilliant blue.

Enzyme purification. The results of a typical purification of *T. maritima* DHFR from 25 g (wet mass) *E. coli* pTM9 cells, cultivated as described in Materials and Methods, are summarized in Table 2. Owing to the high amount of *T. maritima* DHFR in the cells, its high thermal stability compared to *E. coli* proteins, and the high specificity of methotrexate-agarose for DHFRs, only two purification steps were required to obtain pure recombinant

Table 3. Gel-filtration FPLC chromatography of pure DHFR–H_2-folate complex. The column was first calibrated in each buffer using protein standards from Pharmacia. Proteins were detected by measuring the absorbance at 280 nm and DHFR activity was assayed under standard conditions (see Materials and Methods).

Elution buffer	Mass	Structure
	Da	
Citrate/HCl, pH 4.3	20 400	monomer
Citrate/HCl, pH 4.3 + 0.1 M NaCl	33 000	dimer
Mes, pH 6.5 + 0.1 M NaCl	36 350	dimer
Potassium phosphate, pH 7.5	39 000	dimer
Sodium carbonate, pH 10.3	33 300	dimer
Sodium carbonate, pH 10.3 + 0.1 M NaCl	36 550	dimer

DHFR. The heat-treatment step inactivated *E. coli* DHFR so that pure *T. maritima* DHFR−H_2-folate could be isolated in the subsequent affinity-chromatography step. A high pH (10.3) was necessary to release the enzyme from the methotrexate-agarose resin. The purification procedure resulted in 20-fold purification of *T. maritima* DHFR to homogeneity (Fig. 1), with a final yield of 67%. The specific activity of the final *T. maritima* DHFR preparation was 173 U/mg. In this particular purification, overexpressed *T. maritima* DHFR represented approximately 5% of the total protein content in the crude extract.

T. maritima apo-DHFR was also purified in two steps; heat treatment of crude extracts (as described above), followed by cation-exchange chromatography using a Poros 20 HS strong cation-exchange resin. Small quantities of some high molecular mass proteins co-eluted with *T. maritima* DHFR from the cation exchange resin. Initial attempts to separate these components by gel-filtration chromatography were unsuccessful due to problems with aggregation of apo-DHFR (see results for DLS). However, by retaining only those fractions with highest DHFR activity at the peak of the *T. maritima* DHFR elution profile, it was possible to obtain >95% pure apo-DHFR. This material was used for subsequent biophysical measurements. Since large quantities of apo-DHFR were discarded in this procedure, no estimate of yield of pure protein has been made for this procedure. However, typically several milligrams pure protein could be obtained from 1 litre culture.

Molecular mass, subunit structure, and N-terminal amino acid sequence determination. The molecular mass of *T. maritima* DHFR obtained by both affinity chromatography and cation-exchange chromatography procedures was determined by electrospray ionization mass spectrometry. The molecular mass of the protein was found to be 19 200 ± 3 Da in both cases. These experimental results are in excellent agreement with the expected molecular mass of 19 203 Da, based on the deduced amino acid sequence of the protein.

Polyacrylamide gel electrophoresis in denaturing conditions (SDS/PAGE) of pure *T. maritima* DHFR revealed two major bands (Fig. 1) at 19.5 kDa and 33 kDa. These could correspond to a monomeric and a dimeric structure, respectively, of the enzyme. Indeed, thermostable enzymes are often more resistant to denaturing agents such as SDS than mesophilic proteins. In order to investigate this, the two bands obtained by SDS/PAGE were submitted to Edman degradation; both N-terminal amino acid sequences were identical (AKVIFVLAMDV) and corresponded to the N-terminus predicted from the nucleotide sequence of *dyrA*. Thus, the bands do indeed correspond to a monomeric and dimeric form of the protein. Similar reassociation of monomers after SDS denaturation of a thermostable enzyme

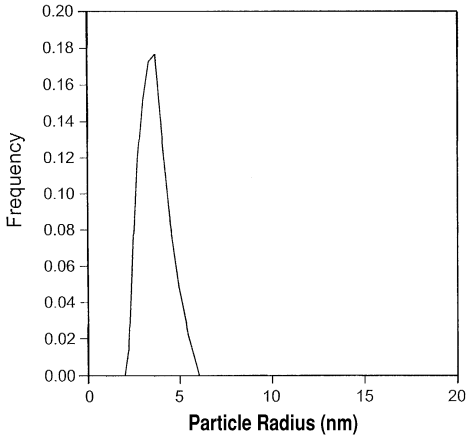

Fig. 2. Protein size analysis by DLS. The sample contained ≈5 mg/ml *T. maritima* DHFR-methotrexate complex in 75 mM KH_2PO_4/K_2HPO_4, pH 6.5, at ambient temperature. The main species in solution has a hydrodynamic radius of 4.7 nm and there is a minor component with a radius of ≈16.5 nm.

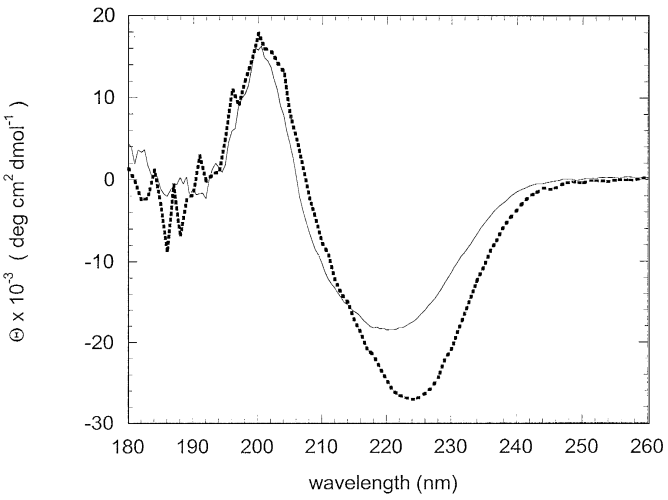

Fig. 3. CD spectra. Far-ultraviolet CD spectra of *T. maritima* apo-DHFR (solid line) and DHFR-methotrexate complex (dashed line). Samples contained ≈5 mg/ml protein in 75 mM KH_2PO_4/K_2HPO_4, pH 6.5, at ambient temperature.

was also observed for ornithine carbamoyltransferase of *Pyrococcus furiosus* [43].

As DHFRs from other species are usually monomers or part of a bifunctional DHFR-TS enzyme, we further investigated oligomerization of *T. maritima* DHFR by gel-filtration chromatography (Table 3). Based on these experiments, recombinant *T. maritima* DHFR generally forms a dimer of two 19-kDa subunits. A monomeric form of the enzyme is observed only at low pH (4.3) in the absence of NaCl. Thus, the pH of the eluting buffer affects the quaternary structure of the enzyme and NaCl promotes dimer formation at both low and high pH values.

Dynamic light scattering measurements. DLS measurements were made to determine the hydrodynamic radius of *T. maritima* apo-DHFR and of the complexes DHFR−H_2-folate and DHFR-methotrexate in solution. The solution of apo-DHFR was very slightly cloudy and DLS detected small amounts of aggregated material with a broad range of sizes. DLS is extremely sensitive to the presence of large particles because these scatter light much more strongly than small particles. Since large species do-

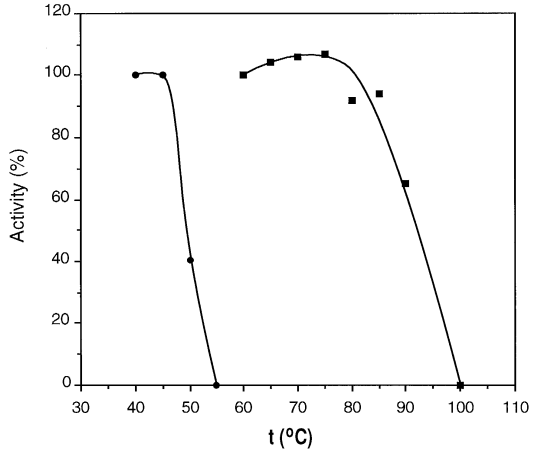

Fig. 4. Thermal stability of *E. coli* DHFR and *T. maritima* DHFR. The residual DHFR activity was assayed at 37°C after 15 min incubation of a crude extract at different temperatures; *E. coli* non-recombinant cells giving the DHFR activity due to the enterobacterial enzyme (●) and *E. coli* recombinant cells harbouring pTM9 plasmid giving the DHFR activity due to the expression of the DHFR encoding gene of *T. maritima* in *E. coli* (■). Data are expressed relative to the activity measured in the extract that was not incubated, deducing the *E. coli* DHFR activity from the total DHFR activity in *E. coli* recombinant cells.

Table 4. Thermal stability of the pure *T. maritima* DHFR at 80°C. The pure enzyme was in 50 mM potassium phosphate, pH 7.5.

[Enzyme]	Effector added	Half-life
mg/ml	M	min
0.2	none	68−72
0.1	none	58−62
0.02	none	60−64
0.1	NADPH (10^{-4})	>360
0.1	H_2-folate (10^{-4})	>240
0.1	NaCl (0.1)	59−63
0.1	urea (1)	26−28

minated the scattering profile of the apo-DHFR sample, it was not possible to determine the hydrodynamic radius for apo-DHFR. Similar aggregation of apo-DHFR has been observed for human DHFR (Nirmala, N. R., unpublished results).

In contrast to apo-DHFR, DHFR−H_2-folate and DHFR-methotrexate complexes formed clear solutions, in which the main species could be measured and had hydrodynamic radiuses of 5.0 nm and 4.9 nm (Fig. 2). Both solutions also contained very small quantities of aggregated material (size in the order of micrometers); this material precipitated over a period of several days when the solutions were kept at ambient temperature. The radii for DHFRs in crystal structures are 2−2.5 nm ([44] and references therein), which are about 50% the size of radii measured for *T. maritima* DHFR by DLS.

Circular dichroism measurements. Far-ultraviolet CD measurements were performed in order to investigate the secondary structure of *T. maritima* DHFR in solution. Spectra were acquired for both apo-DFHR and DHFR-methotrexate complexes (Fig. 3). The spectra of *T. maritim*a DHFR are remarkably similar to corresponding spectra for *E. coli* DHFR [45, 46]. Overall, the spectra for *T. maritima* DHFR are also very similar to spectra for *Lactobacillus casei* DHFR [47] and chicken liver DHFR [48], although there are some minor differences.

A quantitative estimate of the secondary structure of apo-DHFR was obtained using the k2d program, which uses a neural network-based method to predict protein secondary structure based on CD data (see Materials and Methods). According to this method, apo-DHFR consists of approximately 14% helix, 38% β sheet and 48% coil structure. The prediction was within the acceptable error limits as reported by the program. The predicted secondary structure of *T. maritima* DHFR can be compared with the known secondary structure of DHFRs in crystal structures: *E. coli* DHFR (pdb code 1ra9), 25% helix, 31% β-sheet and 44% coil; *Lactobacillus casei* DHFR (pdb code 3dfr), 24% helix, 31% β sheet and 45% coil; chicken liver DHFR (pdb code 8dfr), 23% helix, 32% β sheet and 45% coil; human DHFR (pdb code 1dhf), 22% helix, 31% β sheet and 47% coil. Thus, the predicted secondary structure of *T. maritima* DHFR is very similar to the known secondary structure of other bacterial and eukaryotic DHFRs.

Thermal properties of the enzyme. The thermal stability of *T. maritima* DHFR was investigated by measuring residual activity after incubating crude extract at different temperatures (Fig. 4). 100% activity was retained after heating the extract for 15 min at 75°C, whereas *E. coli* DHFR was completely inactivated by a 15-min incubation at 55°C. 65% *T. maritima* DHFR activity remained after 15 min incubation at 90°C, and boiling for 15 min resulted in complete inactivation (Fig. 4).

The thermal stability of pure DHFR was investigated at 80°C (*T. maritima* optimal growth temperature). The stability of the pure enzyme was similar to that of enzyme in the crude extracts and did not appear markedly concentration-dependent (Table 4). The presence of either substrate during the heat treatment strikingly protected the enzyme and this effect was more pronounced for NADPH than for H_2-folate. In contrast, the half-life at 80°C was reduced by a factor two in 1 M urea (Table 4). Addition of NaCl resulted in a biphasic denaturation process (data not shown); 40% of the activity was lost during the first 30 min incubation (half-life identical to the control, Table 4), but the 60% remaining activity was stable at least until 90 min. This feature could be caused by increased formation of dimer in the presence of NaCl.

pH dependence of enzyme activity and solubility. *T. maritima* DHFR activity was measured as a function of pH at 37°C and at 60°C, as described in Materials and Methods. The optimal pH for activity of *T. maritima* DHFR is about 6.5 at 37°C, and about 6.3 at 60°C. These pHs are quite similar to optimal pHs for DHFRs from other species (Table 5). However, in contrast to DHFRs from human, chicken and *E. coli* which have two maxima, the pH profile for *T. maritima* DHFR has only one maximum.

The solubility of purified, concentrated DHFR−H_2-folate is pH-dependent. This complex is very soluble at basic pH (pH 8.5−10.3). At lower pH, however, it precipitates in a reversible manner. The precipitated complex could be resolubilized by raising the pH (e.g. by using sodium carbonate, pH 10.3).

The isoelectric pHs of apo-DHFR, DHFR-methotrexate and DHFR-methotrexate-NADPH were investigated using IEF gel electrophoresis (Table 5). Due to technical difficulties in measuring pI values greater than pH 9, it was only possible to determine that the pI of apo-DHFR was greater than pH 9. Ligand binding resulted in a lowering of the pI of the apo-protein to pH 8.1 for DHFR-methotrexate and to 7.0 for DHFR-methotrexate-NADPH. The lowered pIs for the complexes are similar to results obtained for other DHFRs, however, all pI values for *T. maritima* DHFR are considerably higher than corresponding pIs measured for other DHFRs (see Table 5). Interestingly, the pI of

Table 5. Kinetic and Biochemical parameters of DHFRs from different sources.

Source and references	K_m for		IC_{50} for		Optimal pH	pI			
	H_2-folate	NADPH	metho-trexate	trimetho-prim		apo-DHFR	DHFR-metho-trexate	DHFR−H_2-folate	DHFR-metho-trexate-NADPH
	μM								
Toxoplasma gondii [51]	0.6	0.5		8	6.4				
Pneumocystis carinii [52, 53]	2.3	3.0	0.0001	20	7.0				
Candida albicans [54]	4.0	3.0			6.3	7.1			
Chicken [48]	0.2	1.8			4.0 & 7.4	8.4		7.4	5.5
Human [28, 53, 55, 56]	0.036−0.12	0.25−0.16	0.08	2−300	4.5 & 7.5	7.7		6.2	
Lactobacillus casei [57]	1.5	20.7							
Escherichia coli [13, 29, 56, 58]	0.27−9.0	1.05−4.4	0.003	0.008−0.05	4.0 & 7.0	4.7			
Thermotoga maritima (this study)	0.3	4.0	0.07	300	6.5	>9	8.1		7.0

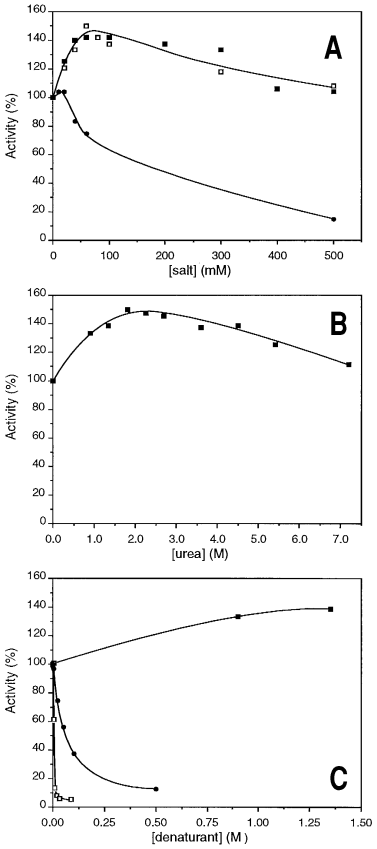

Fig. 5. Effect of inorganic salts and of denaturing agents on the activity of the pure *T. maritima* DHFR-H_2-folate complex. The DHFR activity was assayed under standard conditions in the presence of the following different concentrations of inorganic salts: (a) NaCl (■), KCl (□) or $CaCl_2$ (●); denaturing agents (b) and (c); urea (b and c, ■), SDS (c, □) or guanidine hydrochloride (c, ●). Data are expressed relative to the activity measured in the absence of effectors.

T. maritima DHFR is more similar to those of vertebrate DHFRs than bacterial DHFR.

Kinetic properties of the enzyme. The K_m values for both substrates were determined using partially purified enzyme (first step of purification). Due to the limit of sensitivity of the assay, the very low K_m values are only approximate. The K_m for NADPH is ≈4 μM while that for H_2-folate is ≈0.3 μM. These values are similar to the K_m values of DHFRs from other species (Table 5).

Preliminary experiments showed that *T. maritima* DHFR exhibits hysteretic behaviour, as has been observed for *E. coli* DHFR [29, 49]. When the reaction was initiated by adding NADPH or enzyme solution, a linear consumption of substrates with time was observed. However, when the enzyme was incubated with NADPH (for about 10 s) and the reaction initiated by adding H_2-folate, the reaction rate increased with time (data not shown). This kind of kinetic behaviour was also observed by Baccanari and Joyner [50] for *E. coli* DHFR, although Penner and Frieden [50] did not observe hysteretic behaviour for *E. coli* DHFR incubated with either substrate. As for the enzyme from *E. coli* [50], the hysteretic latency of *T. maritima* DHFR diminished with increasing enzyme concentration.

In order to investigate the affinity of *T. maritima* DHFR for inhibitors of DHFRs, *in vitro* inhibition experiments were performed on pure apo-DHFR. IC_{50} values for different inhibitors were determined under standard conditions. The IC_{50} values are ≈0.07 μM for methotrexate and ≈300 μM for trimethoprim. Compared to IC_{50} concentrations for DHFRs from other sources

Table 6. Amino acid composition of DHFRs from different sources. 38 protein sequences for DHFRs were obtained from all *dyr* sequence entries reported in the Genbank and EMBL databases. Partial sequences were not included, and the TS encoding part was eliminated from the sequences corresponding to DHFR-TS bifunctional enzymes. Amino acid compositions were calculated using the SAPS-server for statistical analysis of protein sequences [60] available at http://ulrec3.unil.ch/software/SAPS__form.html.

Source of the sequences	Number of sequences	(L+V+I+M+F) hydrophobic residues		(R+K)/(D+E) charged residues average ratio
		average	range	
		%		
Higher eukaryotes	10	30.5	28.6−31.7	1.0
Fungi and protozoan	11	29.1	26.2−31.2	1.2
Bacteria	15	30.3	27.6−34.9	0.8
Halobacterium volcanii	1	24.1		0.5
Thermotoga maritima	1	36.0		1.2
Total	38	30.0	24.1−36.0	

(Table 5), the IC_{50} value for methotrexate is relatively high, and that for trimethoprim is elevated compared to that of bacterial *E. coli* DHFR. The results for *T. maritima* DHFR may, however, be deceptively high due to assays being performed at 37 °C, far from the optimal temperature for activity. Also, methotrexate is an inhibitor 4000-fold more potent *in vitro* than trimethoprim. However, as described above, the effect of these inhibitors on the growth of *E. coli* pTM9 was comparable. It is thus likely that trimethoprim enters the cells more easily.

Effect of salts and denaturing agents on enzyme activity. It has been observed previously that vertebrate DHFRs and the protozoan DHFR from *Toxoplasma gondii* can be activated by a diverse group of agents, such as inorganic salts and chaotropes ([59] and references therein, [51]). Since *T. maritima* DHFR is a representative of one of the oldest line of descent among eubacteria and its properties are similar to both eukaryotic and prokaryotic DHFRs ([23] and this paper), the effects on enzyme activity of NaCl, KCl, and $CaCl_2$ as well as of urea, SDS and guanidine hydrochloride were investigated.

T. maritima DHFR is activated 1.4-fold at concentrations of NaCl and KCl of 40−200 mM (Fig. 5a) and is as active in the presence of 500 mM salt as in the absence of salt. In contrast, $CaCl_2$ inhibits enzyme activity at concentrations above 20 mM (Fig. 5a).

As for the DHFRs from chicken liver [59] and from *T. gondii* [51], *T. maritima* DHFR activity increases in the presence of urea (Fig. 5b), however the effect is less pronounced (1.5-fold) than for the eukaryotic DHFRs (4-fold and 5-fold). *T. maritima* DHFR is more active in 7 M urea than in the absence of this denaturing agent. In contrast, a decrease in activity (Fig. 5c) was observed in the presence of low concentrations of SDS (> 7 mM) or guanidine hydrochloride (> 10 mM).

Amino acid composition. The amino acid compositions of DHFRs representing all the major kingdoms were compared with that of *T. maritima* DHFR. In spite of the low identity between DHFRs, some interesting features were observed. The thermostable DHFR from *T. maritima* contains the highest proportion of hydrophobic residues (L, V, I, M, and F) among all other known DHFRs (Table 6). However, in *T. maritima* DHFR as well as in almost all fungal and protozoan DHFRs and several other eukaryotic DHFRs, the amount of positively charged residues (R and K) is higher than the amount of negatively charged residues (D and E), resulting in an excess of positive charges. In contrast, in all the bacterial DHFRs, except for *Mycoplasma* species, the inverse situation is observed (Table 6). The large excess of negatively charged residues observed in the DHFR from *Halobacterium volcanii* (the only archaeal DHFR characterized up to now) has to be related to the halophily of this species.

DISCUSSION

T. maritima DHFR was expressed in *E. coli* using the pET3a expression vector. The enzyme was purified to homogeneity from recombinant cells by a two-step purification procedure, and characterized for a number of biochemical and biophysical properties.

As shown previously, *T. maritima* DHFR exhibits a typically thermophilic temperature profile [23]. The protein is intrinsically thermostable; its stability did not show any striking concentration dependence, but the presence of substrates (NADPH or H_2-folate) markedly improved enzyme stability, even at a rather low concentration.

Based on molecular-size measurements by gel-filtration chromatography, DHFR−H_2-folate complex appears to exist primarily in a dimeric form under most solution conditions. These results differ from those obtained for other DHFRs, which have been found to be monomeric. Measurements of hydrodynamic radii of *T. maritima* DHFR by DLS showed that the radius of the enzyme is roughly twice that expected from crystal structures of various monomeric DHFRs. These data also suggest that *T. maritima* DHFR forms a dimer in solution. The dimerization could have some bearing on the thermostability. Oligomerization has been proposed as a general mechanism by which proteins may increase their stability in thermophilic organisms [61, 62].

The far-ultraviolet CD spectra obtained for *T. maritima* DHFR are very similar to corresponding spectra for *E. coli*, *L. casei* and chicken liver DHFRs. In addition, the predicted secondary structure of *T. maritima* DHFR based on the CD spectra is very similar to the known secondary structure of bacterial and eukaryotic DHFRs in crystal structures. Thus, despite the rather low sequence similarity between *T. maritima* DHFR and other DHFRs [23], and the dimeric state of *T. maritima* DHFR versus the monomeric state of other DHFRs, the secondary structure of *T. maritima* DHFR in solution seems to be very similar to the structures of DHFRs from other species. These results are in agreement with the secondary structure prediction for *T. maritima* DHFR obtained by the program PhDPredict which bases secondary-structure predictions on alignments of homologous proteins [63, 64]. According to this prediction, residues in all the secondary-structural elements observed in other DHFRs are strongly conserved in *T. maritima* DHFR. Thus, all the above results suggest that dimerization probably causes little change in the secondary structure of the protein.

It is known from X-ray crystallography that binding of H_2-folate and methotrexate causes little structural change in both bacterial and eukaryotic DHFRs ([44] and references therein). Since similar and rather limited changes occur in the CD spectra of *T. maritima* DHFR, *L. casei* DHFR and *E. coli* DHFR upon ligand binding, it is likely that binding also causes little change in the structure of *T. maritima* DHFR.

The reaction catalyzed by *T. maritima* DHFR shows hysteretic behaviour for the H_2-folate-initiated reaction. Non-linear kinetics have also been observed for *E. coli* DHFR [49, 50]. The hysteretic phenomenon implies that there are two coexisting forms of the enzyme, one predominant in the absence of the substrate, and the other predominant in the presence of the substrate. This kind of kinetic behaviour requires slow interconversion between two forms of the enzyme which differ in their enzymatic activity [65]. It is possible that this interconversion involves oligomerization of *T. maritima* DHFR, although it may also be caused by slow conformational changes in the active site; for example, Bystroff and Kraut [66] observed conformational changes in *E. coli* DHFR upon the binding of NADPH. However, enzyme-concentration dependency of hysteresis is usually indicative of a polymerization step with the monomer being the less active enzyme species [49].

Interestingly, *T. maritima* DHFR is activated by urea, a property of vertebrate DHFRs [59] that has also been observed for the protozoan DHFR from *T. gondii* [51], but never for a bacterial DHFR. The structural basis for this activation is not known; however, based on trypsin digestions and fluorescence measurements, Fan et al. [59] have proposed that the activation of chicken liver DHFR in dilute denaturants is accompanied by a loosening up of the protein structure, particularly in the vicinity of the active site.

As *T. maritima* DHFR is activated by KCl or NaCl, even at high concentration, and inhibited at low concentration of $CaCl_2$, monovalent cations are probably responsible for activation. Acti-

vation of DHFRs by inorganic salts has often been observed [51, 55, 57, 59]. Contrary to urea, NaCl did not reduce the thermal stability of *T. maritima* DHFR, thus the mechanism of activation by NaCl is likely to be different than that by urea.

In conclusion, *T. maritima* DHFR is the first thermophilic DHFR to be characterized. It resembles in many ways both eukaryotic and bacterial DHFRs, consistent with its phylogeny (on the basis of 16 S RNA comparisons) as one of the most ancient lines of descent not only in the Bacterial domain but in the living world at large. This DHFR also has some unique properties, it forms a dimer under most conditions, has a high thermal stability and a high content of hydrophobic residues. It will be very interesting to determine the tertiary structure of *T. maritima* DHFR, these studies are in progress. Knowledge of the structure of the protein will provide insights into the phylogeny of DHFRs and the role of dimerization in thermostability and thermophily.

The assistance of Dr F. R. Hallett for DLS measurements and A. Doherty-Kirby for mass spectrometry measurements is gratefully acknowledged. We thank D. Gigot for performing FPLC chromatography experiments, J.-P. ten Have for his assistance in computing and in the layout of figures. Prof. P. Falmagne and R. Wattiez from the University of Mons for the N-terminal amino acid sequences determinations are acknowledged. This work was supported by the European Programme for Biotechnology, the Belgian Foundation for Joint and Fundamental Research (FKFO), the Flemish Action Programme for Biotechnology, a Concerted Action between the Belgian State and the free University of Brussels (VUB), and the Natural Sciences and Engineering Research Council of Canada.

REFERENCES

1. Huber, R., Langworthy, T. A., König, H., Thomm, M., Woese, C. R., Sleytr, U. B. & Stetter, K. O. (1986) *Thermotoga maritima* sp.nov. represents a new genus of unique extremely thermophilic eubacteria growing up to 90 °C, *Arch. Microbiol. 144*, 324–333.
2. Huber, R. & Stetter, K. O. (1992) The Thermotogales, in *Thermophilic* bacteria (Kristjansson, J. K., ed.) pp. 185–194, CRC Press, Inc., London.
3. Burggraf, S., Olsen, G. J., Stetter, K. O. & Woese, C. R. (1992) A phylogenetic analysis of *Aquifex pyrophilus*, *Syst. Appl. Microbiol. 15*, 352–356.
4. Rehaber, V. & Jaenicke, R. (1992) Stability and reconstitution of D-glyceraldehyde-3-phosphate dehydrogenase from the hyperthermophilic eubacterium *Thermotoga maritima*, *J. Biol. Chem. 267*, 10999–11006.
5. Wetmur, J. G., Wong, D. M., Ortiz, B., Tong, J., Reichert, F. & Gelfand, D. H. (1994) Cloning, sequencing, and expression of RecA proteins from three distantly related thermophilic eubacteria, *J. Biol. Chem. 269*, 25928–25935.
6. Winterhalter, C. & Liebl, W. (1995) Two extremely thermostable xylanases of the hyperthermophilic bacterium *Thermotoga maritima* MSB8, *Appl. Env. Microbiol. 61*, 1810–1815.
7. Blamey, J. M., Mukund, S. & Adams, M. W. (1994) Properties of a thermostable 4Fe-ferredoxin from the hyperthermophilic bacterium *Thermotoga maritima*, *FEMS Microbiol. Lett. 121*, 165–169.
8. Blamey, J. M. & Adams, M. W. (1994) Characterization of an ancestral type of pyruvate ferredoxin oxidoreductase from the hyperthermophilic bacterium, *Thermotoga maritima*, *Biochemistry 33*, 1000–1007.
9. Blakley, R. L. (1984) Chemistry and biochemistry of folate in *Folates and pterins* (Blakley, R. L. & Benkovic, S. L., eds) vol. 1, pp. 191–253, John Wiley & Sons, New York.
10. Huennekens, F. M. (1996) In search of dihydrofolate reductase, *Protein Sci. 5*, 1201–1208.
11. Kuyper, L. F. (1989) in *Computer-aided drug design: methods and applications* (Perun, T. J. & Propst, C. L., eds) pp. 327–369, Marcel Dekker, Inc., New York.
12. Roth, B. & Stammers, D. K. (1992) in *The design of drugs to macromolecular targets* (Beddell, C. R., ed.) pp. 85–118, John Wiley & Sons Ltd, New York.
13. Hartman, P. G. (1993) Molecular aspects and mechanism of action of dihydrofolate reductase inhibitors, *J. Chemotherapy 5*, 369–376.
14. Huennekens, F. M. (1994) The methotrexate story: a paradigm for development of cancer chemotherapeutic agents, *Adv. Enzyme Regul. 34*, 397–419.
15. Hussain, A., Lewis, D., Sumbilla, C., Lai, L. C., Melera, P. W. & Inesi, G. (1992) Coupled expression of Ca^{2+} transport ATPase and a dihydrofolate reductase selectable marker in a mammalian cell system, *Arch. Biochem. Biophys. 296*, 539–546.
16. Sirawaraporn, W., Cao, M., Santi, D. V. & Edman, J. C. (1993) Cloning, expression, and characterization of *Cryptococcus neoformans* dihydrofolate reductase, *J. Biol. Chem. 268*, 8888–8892.
17. Israel, D. I. & Kaufman, R. J. (1993) Dexamethasone negatively regulates the activity of a chimeric dihydrofolate reductase/glucocorticoid receptor protein, *Proc. Natl Acad. Sci. USA 90*, 4290–4294.
18. Donald, R. G. K. & Roos, D. S. (1993) Stable molecular transformation of *Toxoplasma gondii*: a selectable dihydrofolate reductase-thymidylate synthase marker based on drug-resistance mutations in malaria, *Proc. Natl Acad. Sci. USA 90*, 11703–11707.
19. Fujita, S., Koguma, T., Ohkawa, J., Mori, K., Kohda, T., Kise, H., Nishikawa, S., Iwakura, M. & Taira, K. (1997) Discrimination of a single base change in a ribozyme using the gene for dihydrofolate reductase as a selective marker in *Escherichia coli*, *Proc. Natl Acad. Sci. USA 94*, 391–396.
20. Leszczynska, K., Bolhuis, A., Leenhouts, K., Venema, G. & Ceglowski, P. (1995) Cloning and molecular analysis of the dihydrofolate reductase gene from *Lactococcus lactis*, *Appl. Env. Micobiol. 61*, 561–566.
21. Roos, D. S. (1993) Primary structure of the dihydrofolate reductase-thymidylate synthase gene from *Toxoplasma gondii*, *J. Biol. Chem. 268*, 6269–6280.
22. Zusman, T., Rosenshine, I., Boehm, G., Jaenicke, R., Leskiw, B. & Mevarech, M. (1989) Dihydrofolate reductase of the extremely halophilic archaebacterium *Halobacterium volcanii*, *J. Biol. Chem. 264*, 18878–18883.
23. Van de Casteele, M., Legrain, C., Wilquet, V. & Glansdorff, N. (1995) The dihydrofolate reductase-encoding gene *dyrA* of the hyperthermophilic bacterium *Thermotoga maritima*, *Gene* (*Amst.*) *158*, 101–105.
24. Dale, G., Broger, C., Hartman, P. G., Langen, H., Page, M. G. P., Then, R. L. & Stüber, D. (1995) Characterization of the gene for the chromosomal dihydrofolate reductase (DHFR) of *Staphylococcus epidermidis* ATCC 14990: the origin of the trimethoprim-resistant S1 DHFR from *Staphylococcus aureus*? *J. Bacteriol. 177*, 2965–2970.
25. Fierke, C. A., Johnson, K. A. & Benkovic, S. J. (1987) Construction and evaluation of the kinetic scheme associated with dihydrofolate reductase from *Escherichia coli*, *Biochemistry 26*, 4085–4092.
26. Margosiak, S. A., Appleman, J. R., Santi, D. V. & Blakley, R. L. (1993) Dihydrofolate reductase from the pathogenic fungus *Pneumocystis carinii*: catalytic properties and interaction with antifolates, *Arch. Biochem. Biophys. 305*, 499–509.
27. Thillet, J., Adams, J. A. & Benkovic, S. J. (1990) The kinetic mechanism of wild-type and mutant mouse dihydrofolate reductases, *Biochemistry 29*, 5195–5202.
28. Appleman, J. R., Beard, W. A., Delcamp, T. J., Prendergast, N. J., Freisheim, J. H. & Blakley, R. L. (1990) Unusual transient- and steady-state kinetic behaviour is predicted by the kinetic scheme operational for recombinant human dihydrofolate reductase, *J. Biol. Chem. 265*, 2740–2748.
29. Penner, M. H. & Frieden, C. (1987) Kinetic analysis of the mechanism of *Escherichia coli* dihydrofolate reductase, *J. Biol. Chem. 262*, 15908–15914.
30. Studier, F. W. & Moffatt, B. A. (1986) Use of bacteriophage T7 RNA polymerase to direct selective high-level expression of cloned genes, *J. Mol. Biol. 189*, 113–130.
31. Rosenberg, A. H., Lade, B. N., Chui, D. S., Lin, S.-W., Dunn, J. J. & Studier, F. W. (1987) Vectors for selective expression of

cloned DNAs by T7 RNA polymerase, *Gene* (*Amst.*) *56*, 125−135.
32. Glansdorff, N. (1965) Topography of cotransducible arginine mutations in *Escherichia coli* K-12, *Genetics 51*, 167−179.
33. Brosius, J. & Holy, A. (1984) Regulation of ribosomal RNA promoters with a synthetic *lac* operator, *Proc. Natl Acad. Sci. USA 81*, 6929−6933.
34. Sambrook, J., Fritsch, E. F. & Maniatis T. (1989) *Molecular cloning: a laboratory manual*, 2d edn, Cold Spring Harbor Laboratory, Cold Spring Harbor, NY.
35. Sanger, F., Nicklen, S. & Coulson, A. R. (1977) DNA sequencing with chain-terminating inhibitors, *Proc. Natl Acad. Sci. USA 74*, 5463−5467.
36. Lowry, O. H., Rosebrough, N. J., Farr, A. L. & Randall, R. J. (1951) Protein measurement with the folin phenol reagent, *J. Biol. Chem. 193*, 265.
37. Hallett, F. R., Craig, T., Marsh, J. & Nickel, B. (1988) Particle size analysis: number distributions by dynamic light scattering, *Can. J. Spect. 34*, 63−70.
38. Andrade, M. A., Chacòn, P., Merelo, J. J. & Morán, F. (1993) Evaluation of secondary structure of proteins from UV circular dichroism using an unsupervised learning neural network, *Prot. Eng. 6*, 383−390.
39. Merelo, J. J., Andrade, M. A., Prieto, A. & Morán, F. (1994) Proteinotopic feature maps, *Neurocomputing 6*, 443−454.
40. Filman, D. J., Bolin, J. T., Matthews, D. A. & Kraut, J. (1982) Crystal structures of *Escherichia coli and Lactobacillus casei* dihydrofolate reductase refined at 1.7 Å resolution, *J. Biol. Chem. 257*, 13663−13672.
41. Oefner, C., D'Arcy, A. & Winkler, F. K. (1988) Crystal structure of human dihydrofolate reductase complexed with folate, *Eur. J. Biochem. 174*, 377−385.
42. Davies, J. R. II, Delcamp, T. J., Prendergast, N. J., Ashford, V. A., Freisheim, J. H. & Kraut, J. (1990) Crystal structures of recombinant human dihydrofolate reductase complexed with folate and 5-deazafolate, *Biochemistry 29*, 9467−9479.
43. Legrain, C., Villeret, V., Roovers, M., Gigot, D., Dideberg, O., Piérard, A. & Glansdorff, N. (1997) Biochemical characterization of ornithine carbamoyltransferase from *Pyrococcus furiosus*, *Eur. J. Biochem. 247*, 1046−1055.
44. Kraut, J. & Matthews, D. A. (1987) Dihydrofolate reductase in *Biological macromolecules and assemblies: active sites of enzymes* (Jurnak, F. A. & McPherson, A., eds) vol. 3, pp. 1−71, Wiley, New York.
45. Kuwajima, K., Garvey, E. P., Finn, B. E., Matthews, C. R. & Sugai, S. (1991) Transient intermediates in the folding of dihydrofolate reductase as detected by far-ultraviolet circular dichroism spectroscopy, *Biochemistry 30*, 7693−7703.
46. Kitchell, B. B. & Henkens, R. W. (1978) Effect of temperature on fluorescence and circular dichroism of *Escherichia coli* dihydrofolate reductase and its complexes, *Biochim. Biophys. Acta 534*, 89−98.
47. Hood, K., Bayley, P. M. & Roberts, C. K. (1979) Circular-dichroism studies of ligand binding to dihydrofolate reductase from *Lactobacillus casei* MTX/R, *Biochem. J. 177*, 425−432.
48. Kaufman, B. T. & Kemerer, V. F. (1977) Characterization of chicken liver dihydrofolate reductase after purification by affinity chromatography and isoelectric focusing, *Arch. Biochem. Biophys. 179*, 420−431.
49. Baccanari, D. P. & Joyner, S. S. (1981) Dihydrofolate reductase hysteresis and its effect on inhibitor binding analyses, *Biochem. 20*, 1710−1716.
50. Penner, M. H. & Frieden, C. (1985) Substrate-induced hysteresis in the activity of *Escherichia coli* dihydrofolate reductase, *J. Biol. Chem. 260*, 5366−5369.
51. Trujillo, M., Donald, R. G. K., Roos, D. S., Greene, P. J. & Santi, D. V. (1996) Heterologous expression and characterization of the bifunctional dihydrofolate reductase-thymidylate synthase enzyme of *Toxoplasma gondii*, *Biochemistry 35*, 6366−6374.
52. Delves, C. J., Ballantine, S. P., Tansik, R. L., Baccanari, D. P. & Stammers, D. K. (1993) Refolding of recombinant *Pneumocystis carinii* dihydrofolate reductase and characterization of the enzyme, *Protein Expr. Purif. 4*, 16−23.
53. Edman, J. C., Edman, U., Cao, M., Lundgren, B., Kovacs, J. A. & Santi, D. V. (1989) Isolation and expression of the *Pneumocystis carinii* dihydrofolate reductase, *Proc. Natl Acad. Sci. USA 86*, 8625−8629
54. Baccanari, D. P., Transik, R. L., Joyner, S. S., Fling, M. E., Smith, P. L. & Freisheim, J. H. (1989) Characterization of *Candida albicans* dihydrofolate reductase, *J. Biol. Chem. 264*, 1100−1107.
55. Delcamp, T. J., Susten, S. S., Blankenship, D. T. & Freisheim, J. H. (1983) Purification and characterization of dihydrofolate reductase from methotrexate-resistant human lymphoblastoid cells, *Arch. Biochem. Biophys. 179*, 420−431.
56. Hitchings, G. H. & Burchall, J. J. (1965) Inhibition of folate biosynthesis and function as a basis for chemotherapy, *Adv. Enzymol. 27*, 417−468.
57. Dann, J. G., Ostler, G., Bjur, R. A., King, R. W., Scudder, P., Turner, P. C., Roberts, G. C. & Burgen, A. S. (1976) Large-scale purification and characterization of dihydrofolate reductase from a MTX^R strain of *Lactobacillus casei*, *Biochem. J. 157*, 559−571.
58. Baccanari, D. P., Averett, D., Briggs, C. & Burchall, J. (1977) *Escherichia coli* dihydrofolate reductase: isolation and characterization of two isozymes, *Biochemistry 16*, 3566−3572.
59. Fan, Y. X., Ju, M., Zhou, J. M. & Tsou, C. L. (1996) Activation of chicken liver dihydrofolate reductase by urea and guanidine hydrochloride is accompanied by conformational change at the active site, *Biochem. J. 315*, 97−102.
60. Brendel, V., Bucher, P., Nourbakhsh, I., Blaisdell, B. E. & Karlin, S. (1992) Methods and algorithms for statistical analysis of protein sequences, *Proc. Natl Acad. Sci. USA 89*, 2002−2006.
61. Jaenicke, R., Schurig, H., Beaucamp, N. & Ostendorp, R. (1996) Structure and stability of hyperstable proteins: glycolytic enzymes from hyperthermophilic bacterium *Thermotoga maritima*, *Adv. Protein Chem. 48*, 181−269.
62. Villeret, V., Clantin, B., Tricot, C., Legrain, C., Roovers, M., Stalon, V., Glansdorff, N. & Van Beeumen, J. (1998) The crystal structure of *Pyrococcus furiosus* ornithine carbamoyltransferase reveals a key role for oligomerization in enzyme stability at extremely high temperatures, *Proc. Natl Acad. Sci. USA 95*, 2801−2806.
63. Rost, B. & Sander, C. (1993) Prediction of protein secondary structure at better than 70% accuracy, *J. Mol. Biol. 232*, 584−599.
64. Rost, B. & Sander, C. (1994) Combining evolutionary information and neural networks to predict protein secondary structure, *Prot. Struct. Funct. Genet. 19*, 55−77.
65. Frieden, C. (1970) Kinetic aspects of regulation of metabolic processes, *J. Biol. Chem. 245*, 5788−5799.
66. Bystroff, C. & Kraut, J. (1991) Crystal structure of unliganded *Escherichia coli* dihydrofolate reductase. Ligand-induced conformational changes and cooperativity in binding, *Biochemistry 30*, 2227−2239.